Catalysis Today 175 (2011) 271–275

Contents lists available at ScienceDirect

Catalysis Today

journal homepage: www.elsevier.com/locate/cattod

A density functional theory study on CO_2 capture and activation by graphene-like boron nitride with boron vacancy

Yan Jiao[a,b], Aijun Du[a,*], Zhonghua Zhu[b,**], Victor Rudolph[b], Gao Qing (Max) Lu[c], Sean C. Smith[a,***]

[a] Centre for Computational Molecular Science, Australian Institute for Bioengineering and Nanotechnology, The University of Queensland, Brisbane, QLD 4072, Australia
[b] School of Chemical Engineering, The University of Queensland, Brisbane, QLD 4072, Australia
[c] ARC Centre of Excellence for Functional Nanomaterials, The University of Queensland, Brisbane, QLD 4072, Australia

ARTICLE INFO

Article history:
Received 15 October 2010
Received in revised form 8 February 2011
Accepted 28 February 2011
Available online 31 March 2011

Keywords:
Carbon dioxide
Activation
Graphene-like boron nitride
Boron vacancy

ABSTRACT

First principle calculations for a hexagonal (graphene-like) boron nitride (g-BN) monolayer sheet in the presence of a boron-atom vacancy show promising properties for capture and activation of carbon dioxide. CO_2 is found to decompose to produce an oxygen molecule via an intermediate chemisorption state on the defect g-BN sheet. The three stationary states and two transition states in the reaction pathway are confirmed by minimum energy pathway search and frequency analysis. The values computed for the two energy barriers involved in this catalytic reaction after enthalpy correction indicate that the catalytic reaction should proceed readily at room temperature.

1. Introduction

Carbon dioxide capture and activation is a topic of extensive ongoing research. On one hand, there is a pressing need to reduce CO_2 emissions, while on the other, CO_2 may be viewed and potentially exploited as a nontoxic and renewable feedstock for the production of many chemicals [1,2]. If it could be implemented economically on a large scale, the manufacture of chemicals utilizing carbon dioxide may have some positive effect on the global carbon balance. Previous research on CO_2 activation has mainly focused on how to improve the reaction efficiency and decrease the impractically high conversion temperatures [3,4]. Due to the highly stable nature of carbon dioxide, the development of materials or catalysts for efficient fixation and chemical activation of CO_2 with respect to subsequent chemical transformations is an obvious point of focus. Catalyst support for CO_2 reduction materials should possess properties such as high surface area, good chemical and mechanical stability, good electrical conductivity as well as good catalytic performance.

According to several recent studies, nitrogen atoms incorporated in a system possessing negative charge density behave as the potential active site for carbon dioxide chemisorption [5–8]. Although the hexagonal aluminium nitride structures proposed in our recent work [7,8] show strong binding with carbon dioxide, such structures (while theoretically stable) remain to be synthesized. Hence studies of other more readily synthesized nanomaterials possessing similar chemical functionality are needed in order to explore whether they may exhibit comparable – or better – performance in CO_2 fixation and activation.

Recently, several groups have reported the experimental preparation of hexagonal graphitic boron nitride (g-BN) single layers [9–13]. g-BN formation is reported to be energetically favourable; these structures are mechanically and chemically as robust as their carbon counterparts, i.e. graphene, while exhibiting better thermal conductivity [14]. In passing one note that the successful synthesis of graphene-like boron nitride consistent with theoretical predictions [15] along with other first principle calculations on similar structures [16,17] reveals the importance of computational chemistry in this field.

Similar to its tubular form, i.e. BN nanotubes [18], single-atom vacancies exists in synthesized g-BN. Furthermore, these vacancies could in principle be created in a controllable manner by electron beam irradiation onto g-BN sheets [13]. Unlike in crystalline boron nitride, where nitrogen vacancies are easier to create [19,20], boron vacancies are easier to create in boron nitride nanotubes [14]. Boron vacancies, with edges terminated by doubly coordinated nitrogen atoms, dominate single-atom defects in g-BN [12]. Other theoretical work has also indicated that the single-atom boron vacancy is more easily created in g-BN, being more stable than the equiva-

* Corresponding author. Tel.: +61 7 3346 3972; fax: +61 7 3346 3992.
** Corresponding author. Tel.: +61 7 3365 3528; fax: +61 7 3365 4199.
*** Corresponding author. Tel.: +61 7 3346 3949; fax: +61 7 3346 3992.
E-mail addresses: a.du@uq.edu.au (A. Du), z.zhu@uq.edu.au (Z. Zhu), s.smith@uq.edu.au (S.C. Smith).

0920-5861/$ – see front matter © 2011 Elsevier B.V. All rights reserved.
doi:10.1016/j.cattod.2011.02.043

lent nitrogen vacancy [21]. For these reasons, we examine in this paper the effect of single-atom boron vacancy defects in g-BN on CO_2 fixation and activation.

2. Computational and theoretical details

Our density functional theory calculations of CO_2 adsorption on infinitely large graphene-like boron nitride sheets utilized the *Dmol*^{3} code [22,23] to compute equilibrium geometries, total energies, transition states, and to perform frequency and charge analysis. Electronic exchange correlation was treated using generalized gradient approximation (GGA) [24,25] with the PW91 functional [26]. The positions of all the atoms were fully relaxed until the following convergence criterion are respectively met: 10^{-5} Ha for total energy, 0.002 Ha/Å for force and 0.005 Å for displacement. The self-consistent field computations criterion was chosen to be 10^{-6} Ha. The electronic wave functions were expanded in a 3.5 version double numerical plus polarization basis set (DNP) truncated at a real space cut-off of 4.1 Å. Due to the presence in the models of boron vacancies, all calculations were spin unrestricted. A 5×10^{-4} Ha smearing [27] and 6 Pulay direct inversion of the iterative subspace (DIIS) [28] was applied to the system to facilitate convergence of the electronic structures.

3D periodic boundary conditions were applied to the whole system to simulate the infinitely large g-BN. The size of the vacuum space in-between two sheets was set to be 20 Å to prevent the interaction of atoms with its periodic images. The Brillouin zone for a single cell was sampled by $12 \times 12 \times 1$ special *k*-points. The lattice parameter of the single cell was optimized to 2.516 Å. The supercell was constructed by five such single cells on each side of the lattice except for the (0 0 0 1) direction, and the lattice parameter was 12.580 Å. The *k*-points set for such a supercell was $2 \times 2 \times 1$ during all the calculations including the vacancy model.

The transition state search was conducted by the complete synchronous transit method [29] implemented in *Dmol*^{3} code, which avoids the time-consuming computation of the Hessian matrix. The root-mean-square convergence criterion of the gradient was set to be 0.002 Ha Å^{-1}. All computed stationary points and transition states on the potential energy surface were confirmed by frequency analysis and minimum energy pathway (MEP) search based on Nudged-Elastic Band (NEB) algorithm [30] in *Dmol*^{3} package.

The equation below was used to calculate the adsorption energy of gas molecules onto g-BN.

$$E_{ad} = E_{Sub+gas} - (E_{Sub} + E_{gas}) \quad (1)$$

where $E_{Sub+gas}$ is the total energy of the substrate (g-BN with/without boron vacancy) after gas adsorption, E_{Sub} is the energy of pure substrate, and E_{gas} is the total energy of isolated gas molecule.

The charge distribution on the system was analyzed by the Hirshfeld method [31], and the bond orders were quantified by Mayer bond order analysis [32]. Since *Dmol*^{3} can only calculate bond order on systems with C1 symmetry, the periodicity of the analyzed system was broken first and the resultant dangling bonds were saturated with hydrogen. A geometry optimization with the backbone atom fixed was carried out, followed by the bond order calculation. The electron density difference was generated by subtracting the electron densities of separate adsorbents and adsorbate, i.e. the gas molecule, from the total electron density of the system.

3. Results and discussion

3.1. CO_2 adsorption on perfect g-BN sheet without vacancy

The B–N bond length of our optimized g-BN structure is 1.45 Å, in good accordance with experimental and previous theoretical results [11,33]. The adsorption energy of CO_2 on a pure g-BN sheet is calculated to be −0.05 eV, with the carbon dioxide molecule parallel to the sheet plane and right above one nitrogen atom on the BN sheet. The distance between the carbon of CO_2 and the adjacent nitrogen atom in the g-BN sheet is 3.51 Å. Unlike hexagonal graphene-like single layer aluminium nitride (g-AlN), which forms a chemisorption complex with CO_2 as we reported previously [7], carbon dioxide apparently only physisorbs onto the g-BN sheet. The smaller computed physisorption energy and larger C–N distance compared to the g-AlN case (−0.09 eV and 3.45 Å, respectively) using the same model chemistry may be rationalized by the larger electro-negativity of boron (2.04) compared with aluminium (1.61) [34]. Consequently the electron accumulation at the adsorption center, i.e. the nitrogen atom, is less in g-BN than in g-AlN, resulting in smaller electrostatic interaction between carbon and nitrogen. This results ultimately in a smaller adsorption energy and in fact a qualitatively different mechanism (i.e. physisorption compared with chemisorptions in the case of AlN). Stated in another way, the absence of chemisorption for g-BN interacting with CO_2 may be attributed to insufficient electron density on the nitrogen atom to promote the formation of a covalent bond with the CO_2 carbon.

3.2. Boron vacancy on g-BN

After the creation of a boron vacancy, the geometry and the charge distribution around the vacancy is slightly changed in the fully relaxed structure. The bond length between the three dangling nitrogen atoms with adjacent boron atoms shortened from 1.45 Å to 1.41 Å, which is consistent with previous calculations [35]. The electronic charge possessed by these three nitrogen atoms changed from −0.20 to −0.16 e, while the boron atoms attached to them changed from 0.20 to 0.18 e. Unlike in relaxed graphene with one atom vacancy, in which a pentagon is formed resulting from the paring of two of three unpaired bonds [36,37], the relaxation of the g-BN did not lead to the formation of a pentagonal structure. The optimized geometry for this defected system is perfectly planar.

3.3. CO_2 adsorption onto a g-BN sheet with a single-atom boron vacancy – stationary points

Three stationary points were identified for CO_2 adsorption onto g-BN with a single-atom boron vacancy, corresponding to (i) physisorption, (ii) chemisorption and finally (iii) dissociation of an O_2 molecule. The active site identified for these three states is in all cases the boron vacancy.

The configuration of the physisorption state is similar to CO_2 on a perfect g-BN sheet, except that the carbon atom is right above the vacancy with a distance of 3.24 Å. The planarity of the sheet is not affected by physisorption; the natural linear structure and bond lengths of carbon dioxide are also unaffected. The physisorption energy is −0.10 eV. The physisorption configuration and the larger adsorption energy compared with the perfect g-BN case can be explained as follows. The carbon atom possesses positive charge due to its lower electro-negativity comparing to oxygen and hence it is attracted electrostatically to the triangle formed by negatively charged nitrogen atoms surrounding the vacancy. The absence of the boron atom lessens the repulsive component of the interaction. Upon physisorption the charges on the atoms of these two moieties are not changed.

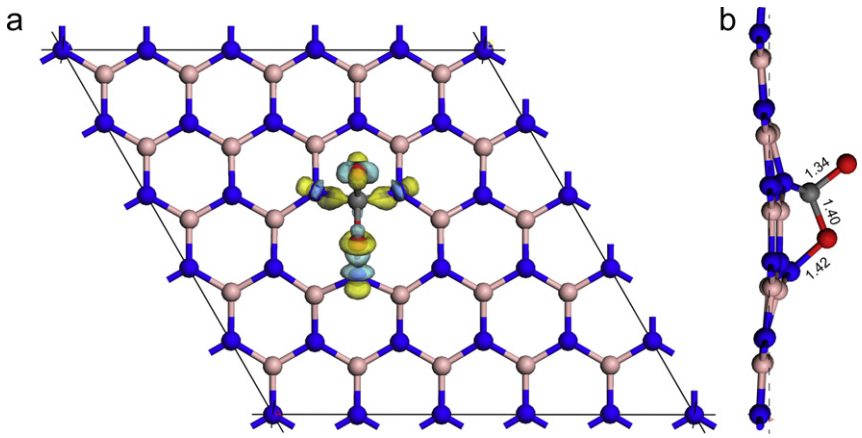

Fig. 1. (a) Structure, electron density difference, and (b) bond length around adsorption center of carbon dioxide chemisorption on g-BN with one boron vacancy. The unit in the figure is in angstrom. The electronic density difference isosurface cut-off value is 0.2 electrons/Å^3. Azure surface corresponds to charge accumulation, and yellow surface corresponds to charge depletion. Atom color code: blue, nitrogen; pink, boron; grey, carbon; and red, oxygen. (For interpretation of the references to color in this figure legend, the reader is referred to the web version of the article.)

The chemisorption energy of CO_2 onto the defect g-BN is −0.62 eV. As shown in Fig. 1, the two moieties are linked by three newly formed covalent bonds: two C–N bonds which are 1.48 Å and one O–N bond whose length is 1.42 Å. A six-membered ring B2N3C and two seven-membered rings B2N3CO are in this way formed. The electron density difference around the adsorption center is also shown in the figure. Electron clouds accumulate in between carbon and nitrogen to facilitate the C–N bond formation. The slight electron depletion around the C–O bond leads to the change in C–O bond order from two to one. The atoms on the BN sheet near the adsorption center move toward the chemisorbed CO_2 which leads to sheet deformation and slight stretching of the BN bonds around the chemisorption center. Charge analysis shows that 0.1 electron transfers from the g-BN to the chemisorbed CO_2 of which the carbon atom acquires 0.1 e^- charge, one of the oxygen atoms gains 0.5 e^- charge, while the other loses 0.5 e^- charge. The formation of the chemisorption state is attributed to the loss of the boron atom which gives room for the positively charged carbon to nestle into the vacancy surrounded by the negatively charged nitrogen atoms.

A third stationary point on the potential energy surface was also identified, in which the carbon atom is implanted into the boron nitride lattice, leaving an oxygen molecule outside and parallel to the g-BN plane. The O–O bond length is 1.29 Å, larger than that of an isolated oxygen molecule calculated on the same model chemistry (1.22 Å). This can be attributed to the interaction of oxygen with the lattice carbon atom. The distance between carbon atom in the BN lattice and the nearest oxygen atom is 1.85 Å. The main g-BN sheet remains essentially planar, with only the carbon atom displaced 0.24 Å out of the plane toward the oxygen molecule. The configuration and electron charge difference is plotted in Fig. 2. At this state, charge on the carbon atom remains the same as the chemisorption one, while the two oxygen atoms both donate electron to the g-BN sheet which makes the oxygen complex more neutral. Comparing to the O_2 totally dissociated state, the lattice-embedded carbon carries more 0.1 e^+ charge because the distance of oxygen complex to the carbon atom is in the range of electron cloud overlap between the two moieties. Comparing to the chemisorption case, the carbon atom and the nitrogen atom that was not connected with are now linked by a newly formed bond. With the cleavage of the two C–O bonds, a new bond between the two oxygen atoms is created. The total energy for this configuration is 1.32 eV lower than the chemisorption one.

3.4. CO_2 adsorption on g-BN sheet with boron vacancy – transition states

Two transition states were found connecting the three stationary points identified in Section 3.3. The first one (TS1) connects the physisorption and chemisorption states of carbon dioxide, with a calculated barrier height of 0.82 eV. The CO_2 molecule bends, with carbon displaced toward the boron vacancy and the C–O bonds stretched to 1.21 Å. One of the three dangling nitrogen atoms moves toward to the carbon of the CO_2, and leads to elongation of the two connected B–N bonds from 1.41 Å to 1.45 Å. Charge analysis shows 0.26 e^- charge transferred from the boron nitride lattice to CO_2 of which the carbon atom and two oxygen atoms acquire 0.09, 0.10, and 0.08 electron.

The dissociation of CO_2 to yield lattice-embedded carbon and adsorbed O_2 is predicted to be achievable following chemisorption of CO_2 onto the defect g-BN via transition state 2 (TS2) with a 0.72 eV barrier. In the transition state, one former C–O bond is broken, yielding CO and another oxygen attached to the dangling nitrogen atom which was not connected with carbon in the chemisorption complex. The carbon carries 0.21 e^+ charge, while the oxygen connected to it carries 0.23 e^- charge, and the oxygen atom connecting to the nitrogen atom carries 0.15 e^- charge.

The single imaginary frequency calculated at TS1 is 467.8i cm^{-1} and that at TS2 is 212.1i cm^{-1}, indicating that the two transition states searched are indeed the connecting local maxima of their respective stationary points which are further confirmed by MEP search. All the identified states are summarized in Fig. 3, which also shows the proposed overall minimum energy reaction path for the adsorption and activation of CO_2 on defect g-BN.

3.5. Energy barrier after enthalpy correction

The energies reported above correspond to only electronic energies under zero Kelvin and as a result the contributions from the vibrational, rotational, and translational energies were not taken into account. Considering explicitly the temperature dependence of the activation barriers gives a more realistic picture of the catalytic reaction. The reaction barriers were corrected by calculating the enthalpy correction and add to the original electronic energies as shown in Table 1.

According to previous study, reactions with a barrier of 21 kcal/mol (∼0.8 eV) or less will proceed readily at room temper-

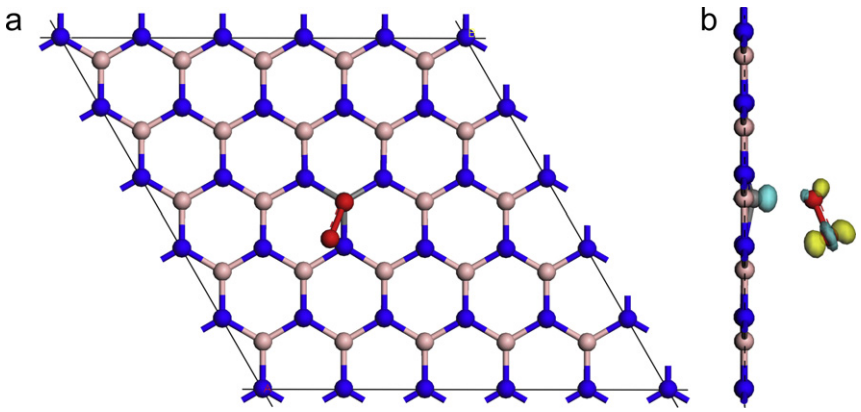

Fig. 2. (a) Structure and (b) electron density difference around adsorption center of oxygen on g-BN with one boron replaced by a carbon atom. The electronic density difference isosurface cut-off value is 0.1 electrons/Å^3. Surface and atom color code: please refer to Fig. 1. (For interpretation of the references to color in this figure legend, the reader is referred to the web version of the article.)

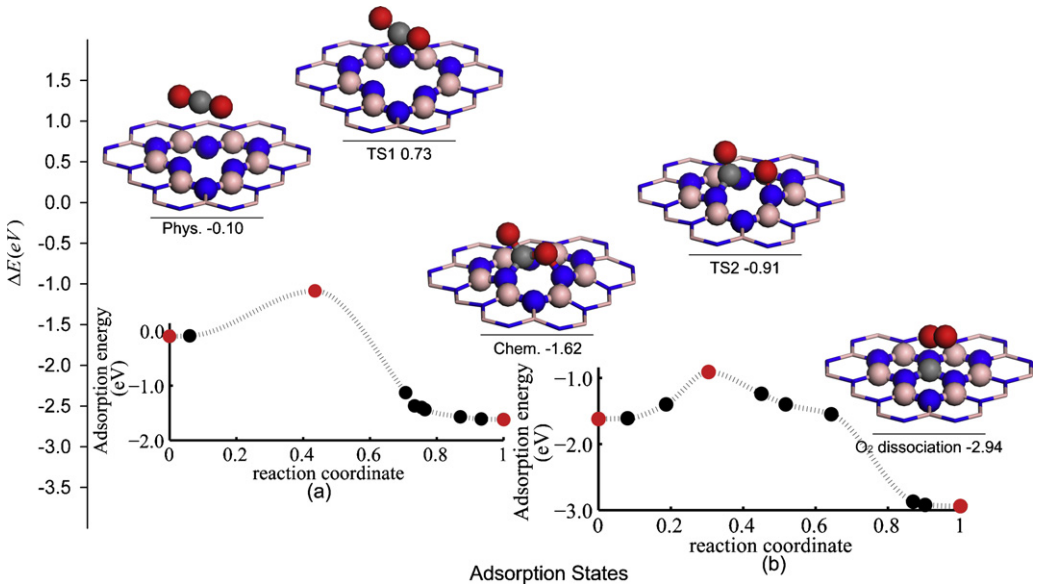

Fig. 3. Catalytic reaction schemes for CO_2 on g-BN layer with one boron vacancy. All the indicated energies are relative to gas phase. The atoms around the adsorption center are represented in ball and stick style, the atoms linking with the adsorption center are represented by stick style, and other atoms are omitted from the figure to keep clarity. Atom color code: please refer to Fig. 1. The MEPs of the reaction are shown as inset (a) and (b). Red dots represent corresponding identified adsorption states and transition states in between. (For interpretation of the references to color in this figure legend, the reader is referred to the web version of the article.)

ature [38]. The corrected reaction barriers at room temperature are within this threshold, indicating that the predicted reaction should be feasible at room temperature. Comparing to a previous study of CO_2 adsorption on defective graphene sheets [39], the current research shows much smaller energy barriers and indicate that these defect-facilitated chemical transformations could proceed under room temperature, suggesting a possible route to CO_2 activation and reduction.

Table 1
Original and corrected barrier of transition states under different temperatures.

Barrier (eV)	No correction	Corrected under different temperatures		
		298.15 K	700 K	1000 K
TS1	0.82	0.76	0.77	0.78
TS2	0.72	0.73	0.69	0.66

4. Conclusions

In summary, we have performed first principle calculations exploring the adsorption of CO_2 onto g-BN with and without single-atom boron vacancies. Unlike the adsorption onto a perfect g-BN plane, carbon dioxide can be captured and activated by g-BN with a boron vacancy, followed by dissociation to produce lattice-embedded carbon and surface-adsorbed molecular oxygen. The strong double bonds in carbon dioxide with energy around 7.7 eV are easily broken due to the presence of the boron vacancy. This reaction suggests a possible route to overcome the obstacle of CO_2 activation, which usually requires very high temperatures. The high surface area, high chemical and mechanical stability suggest that defect-engineered single-layer boron nitride may be a catalyst candidate supposing that the embedded carbon can be removed easily since only the unoccupied boron vacancy site could react with CO_2. Since single-layer g-BN has been successfully synthesized and boron vacancies could in principle be created in a controllable

manner via electron beam irradiation, the reaction scheme we propose in this paper provides an interesting target for experimental validation studies.

Acknowledgements

We acknowledge generous grants of high-performance computer time from the Centre for Computational Molecular Science cluster computing facility at The University of Queensland and the Australian Research Council (LIEF grant LE0882357: A Computational Facility for Multiscale Modeling in Computational Bio and Nanotechnology), and from NCI National Facility in Australia which is supported by the Australian Commonwealth Government. The authors also greatly appreciate financial support from the ARC Discovery Project grant scheme.

References

[1] T. Sakakura, J.C. Choi, H. Yasuda, Chem. Rev. 107 (2007) 2365–2387.
[2] W. Leitner, Coord. Chem. Rev. 153 (1996) 257–284.
[3] H. Arakawa, M. Aresta, J.N. Armor, M.A. Barteau, E.J. Beckman, A.T. Bell, J.E. Bercaw, C. Creutz, E. Dinjus, D.A. Dixon, K. Domen, D.L. DuBois, J. Eckert, E. Fujita, D.H. Gibson, W.A. Goddard, D.W. Goodman, J. Keller, G.J. Kubas, H.H. Kung, J.E. Lyons, L.E. Manzer, T.J. Marks, K. Morokuma, K.M. Nicholas, R. Periana, L. Que, J. Rostrup-Nielson, W.M.H. Sachtler, L.D. Schmidt, A. Sen, G.A. Somorjai, P.C. Stair, B.R. Stults, W. Tumas, Chem. Rev. 101 (2001) 953–996.
[4] J. Ma, N. Sun, X. Zhang, N. Zhao, F. Xiao, W. Wei, Y. Sun, Catal. Today 148 (2009) 221–231.
[5] S.K. Lee, N. Kim, D.G. Ha, S.K. Kim, J. Am. Chem. Soc. 130 (2008) 16241–16244.
[6] C. Villiers, J.P. Dognon, R. Pollet, P. Thuéry, M. Ephritikhine, Angew. Chem. Int. Ed. 49 (2010) 3465–3468.
[7] Y. Jiao, A. Du, Z. Zhu, V. Rudolph, S.C. Smith, J. Phys. Chem. C 114 (2010) 7846–7849.
[8] Y. Jiao, A. Du, Z. Zhu, V. Rudolph, S.C. Smith, J. Mater. Chem. 20 (2010) 10426–10430.
[9] A. Nag, K. Raindogia, K.P.S.S. Hembram, R. Datta, U.V. Wangmare, C.N.R. Rao, ACS Nano 4 (2010) 1539–1544.
[10] J.H. Warner, M.H. Rummeli, A. Bachmatiuk, B. Buchner, ACS Nano 4 (2010) 1299–1304.
[11] N. Alem, R. Erni, C. Kisielowski, M.D. Rossell, W. Gannett, A. Zettl, Phys. Rev. B 80 (2009) 155425.
[12] C.H. Jin, F. Lin, K. Suenaga, S. Iijima, Phys. Rev. Lett. 102 (2009) 195505.
[13] J.C. Meyer, A. Chuvilin, G. Algara-Siller, J. Biskupek, U. Kaiser, Nano Lett. 9 (2009) 2683–2689.
[14] D. Golberg, Y. Bando, K. Kurashima, T. Sato, Scr. Mater. 44 (2001) 1561–1565.
[15] A. Zobelli, A. Gloter, C.P. Ewels, G. Seifert, C. Colliex, Phys. Rev. B 75 (2007) 245402.
[16] A.J. Du, S.C. Smith, G.Q. Lu, Chem. Phys. Lett. 447 (2007) 181–186.
[17] A.J. Du, Z.H. Zhu, Y. Chen, G.Q. Lu, S.C. Smith, Chem. Phys. Lett. 469 (2009) 183–185.
[18] A. Zobelli, C.P. Ewels, A. Gloter, G. Seifert, O. Stephan, S. Csillag, C. Colliex, Nano Lett. 6 (2006) 1955–1960.
[19] I. Jiménez, A.F. Jankowski, L.J. Terminello, D.G.J. Sutherland, J.A. Carlisle, Phys. Rev. B 55 (1997) 12025–12037.
[20] I. Jiménez, A. Jankowski, L.J. Terminello, J.A. Carlisle, D.G.J. Sutherland, G.L. Doll, J.V. Mantese, W.M. Tong, D.K. Shuh, F.J. Himpsel, Appl. Phys. Lett. 68 (1996) 2816–2818.
[21] A. Du, Y. Chen, Z. Zhu, R. Amal, G.Q. Lu, S.C. Smith, J. Am. Chem. Soc. 131 (2009) 17354–17359.
[22] B. Delley, J. Chem. Phys. 92 (1990) 508–517.
[23] B. Delley, J. Chem. Phys. 113 (2000) 7756–7764.
[24] J.P. Perdew, K. Burke, M. Ernzerhof, Phys. Rev. Lett. 77 (1996) 3865–3868.
[25] J.P. Perdew, K. Burke, M. Ernzerhof, Phys. Rev. Lett. 78 (1997) 1396.
[26] J.P. Perdew, J.A. Chevary, S.H. Vosko, K.A. Jackson, M.R. Pederson, D.J. Singh, C. Fiolhais, Phys. Rev. B 46 (1992) 6671–6687.
[27] M. Weinert, J.W. Davenport, Phys. Rev. B 45 (1992) 13709–13712.
[28] P. Pulay, J. Comput. Chem. 3 (1982) 556–560.
[29] T.A. Halgren, W.N. Lipscomb, Chem. Phys. Lett. 49 (1977) 225–232.
[30] G. Henkelman, H. Jonsson, J. Chem. Phys. 113 (2000) 9978–9985.
[31] F.L. Hirshfeld, Theor. Chem. Acc. 44 (1977) 129–138.
[32] I. Mayer, Int. J. Quantum Chem. 29 (1986) 477–483.
[33] L. Pauling, Proc. Natl. Acad. Sci. U.S.A. 56 (1966) 1646–1652.
[34] A.L. Allred, J. Inorg. Nucl. Chem. 17 (1961) 215–221.
[35] M.S. Si, D.S. Xue, Phys. Rev. B 75 (2007) 193409.
[36] P.O. Lehtinen, A.S. Foster, Y. Ma, A.V. Krasheninnikov, R.M. Nieminen, Phys. Rev. Lett. 93 (2004) 187202.
[37] E. Barbary, R.H. Telling, C.P. Ewels, M.I. Heggie, P.R. Briddon, Phys. Rev. B 68 (2003) 144107.
[38] D.C. Young, Computational Chemistry: A Practical Guide for Applying Techniques to Real-World Problems, Wiley, New York, 2001.
[39] P. Cabrera-Sanfelix, J. Phys. Chem. A 113 (2009) 493–498.